

Fe-N_x moieties modified hierarchically porous carbons derived from porphyrins for highly effective oxygen reduction reaction

*Zhengping Zhang, Xinjin Gao, Meiling dou, Jing Ji, and Feng Wang**

State Key Laboratory of Chemical Resource Engineering, Beijing Key Laboratory of Electrochemical Process and Technology for Materials, Beijing University of Chemical Technology, Beijing 100029, China. *E-mail: wangf@mail.buct.edu.cn

Table of Contents

- 1. General methods**
- 2. Characterization of porphyrins and NHPC**
- 3. Characterization of Fe-N_x/HPC**
- 4. Catalytic performance for ORR**

1. General methods

Materials. The porphyrin was grown in Xiapu city (Fujian province, China) and purchased from the super market. Hydrochloric acid (HCl), hydrofluoric acid (HF), sulfuric acid (H₂SO₄), potassium hydroxide (KOH), ethanol, methanol and tetrahydrofuran (THF) were purchased from Sinopharm. High purity argon, oxygen and nitrogen gas were bought from Beijing AP BAIF Gases Industry Co. Ltd. Iron (II) phthalocyanine (FePc), Vulcan XC-72 (commercial carbon black), Corporation. Commercial Pt/C (20 wt.%), Nafion solution (5 wt.%) were purchased from TCI, Cabot, Alfa Aesar and DuPont, respectively. Ultrapure water (18.2 MΩ cm) obtained from a water purification system (TTL-6B) without further purity.

Characterization. Field-emission scanning electron microscopy (FE-SEM, JSM-6701/JEOL), transmission electron microscopy (TEM, JSM-2100/JEOL), aberration-corrected high resolution scanning transmission electron microscope (STEM, JEM-ARM200F/JEOL) were used to characterize the morphology and the microstructure. The powder X-ray diffraction (XRD) from 10 degree to 70 degree was determined by using Cu *K*α radiation at 30 KV and 40 mA. Nitrogen adsorption-desorption isotherms were measured on a Quantachrome AUTOSORB-SI instrument, where the Brunauer-Emmett-Teller (BET) and density functional theory (DFT) methods were used to characterize the specific surface areas and pore size distribution. Raman spectra determined the graphitization degree of the samples using Horiba Jobin Yvon LabRam HR800 confocal microscope. The X-ray photoelectron spectrum (XPS) was conducted with the Thermo Fisher Scientific ESCALAB 250. The FT-IR analysis was performed to determine the functional groups using Nicolet 8700/Continuum XL.

Electrochemical measurements. The electrochemical measurements were conducted respectively with an ALS/DY2323 workstation and a CHI760e electrochemical workstation (Chenhua Instruments Co., Shanghai) workstation in a three-electrode system at room temperature. The working electrode was rotating disk electrode (RDE) or rotating ring-disk electrode (RRDE), a Pt wire and a saturated calomel electrode (SCE) were used as the counter and reference electrodes, respectively. The electrocatalyst inks were prepared by adding 10 mg as-prepared electrocatalysts and 2 mL ethanol with 20 μL Nafion (5 wt.%) solutions by means of sonication dispersing for 30 min. The homogeneous

catalyst ink was transferred onto the surface of the glassy carbon electrode and dried at room temperature for 20 min to obtain a catalyst thin film. The commercial Pt/C electrode was prepared with the same method for comparison. The reversible hydrogen electrode (RHE) was calculated by,

$$E(\text{vs. RHE}) = E(\text{vs. SCE}) + E_{\text{SCE}}^0 + 0.0592 \text{ pH}$$

The accelerated durability tests (ADT) were carried out by potential cycles between 0.6 V to 1.1 V vs. RHE in N₂-saturated 0.1 M KOH solution and 0.05 M H₂SO₄ solution for 3,000 cycles at a scan rate of 100 mV s⁻¹. The ORR polarization curves were measured before and after 3,000 potential cycles. In addition, methanol tolerance test was conducted with the measurement of ORR polarization curves in O₂-saturated 0.1 M KOH and 0.05 M H₂SO₄, with or without 1 M methanol. The capacitance (*C_{dl}*) was evaluated by CV measurements at the region from 1 to 1.2 V vs. RHE with different scan rate (10, 20, 40, 60, 80, 100, 120, 140, 160, 180 and 200 mV s⁻¹), in which no apparent Faradaic processes occurred. The Koutecky–Levich (K-L) plots reflecting the relation of current density (*J*⁻¹) versus rotation rate (*ω*^{-1/2}) were constructed according to:

$$J^{-1} = J_k^{-1} + (0.2nFC_{O_2}D_{O_2}^{2/3}\gamma^{-1/6})^{-1}\omega^{-1/2}$$

where *J_k* is the kinetic-limiting current, *n* is the number of electrons transferred per oxygen molecule, *F* is the Faraday constant (96,485 C mol⁻¹), *C_{O2}*, *D_{O2}* and *γ* are the concentration, the diffusion coefficient of oxygen and the kinematic viscosity, respectively, in 0.1 M KOH and 0.05 M H₂SO₄.

For the Tafel plots, the kinetic current (*J_k*) was calculated from the mass-transport correction of RDE by:

$$J_k = \frac{J \times J_d}{J_d - J}$$

where *J_d* is the diffusion limited current density.

The percentage of hydrogen peroxide yield (% *HO₂⁻*) and the corresponding electron transfer number (*n*) was calculated by RRDE data from:

$$\% HO_2^- = 200 \times \frac{I_r/N}{I_d + I_r/N}$$

$$n = 4 \times \frac{I_d}{I_d + I_r/N}$$

where I_d is disk current, I_r is ring current and $N = 0.4$ is the current collection efficiency of the Pt ring.

2. Characterization of porphyra and NHPC

Table S1 Composition analysis of porphyra (under the 800 °C heat treatment in an air atmosphere)

The ICP calculation of porphyra												
Detectable Element	Al	Ca	Co	Fe	K	Mg	Na	Pb	Zn	P	S	Si
Unit	ppm	ppm	ppm	ppm	ppm	ppm	ppm	ppm	ppm	ppm	ppm	ppm
Average Value	0.3385	38.04	0.0028	0.4309	19.52	3.736	1.992	0.0306	0.4473	12.55	21.18	0.6031
Standard Deviation	0.0039	0.63	0.0001	0.0042	0.33	0.093	0.289	0.0203	0.004	0.13	0.24	0.005
%RSD	1.15	1.665	4.481	0.9848	1.671	2.494	14.51	66.38	0.8984	1.102	1.122	0.9984
Rep#1	0.3413	37.59	0.0028	0.4279	19.75	3.671	2.196	0.045	0.4444	12.46	21.01	0.6002
Rep#2	0.3358	38.49	0.0027	0.4339	19.29	3.802	1.787	0.0162	0.4501	12.64	21.35	0.6059
Calculation ($\mu\text{g}/100\text{ g}$)	1.1	123.63	0.09	1.4	63.44	12.14	6.474	0.09	1.43	68.83	40.79	1.96

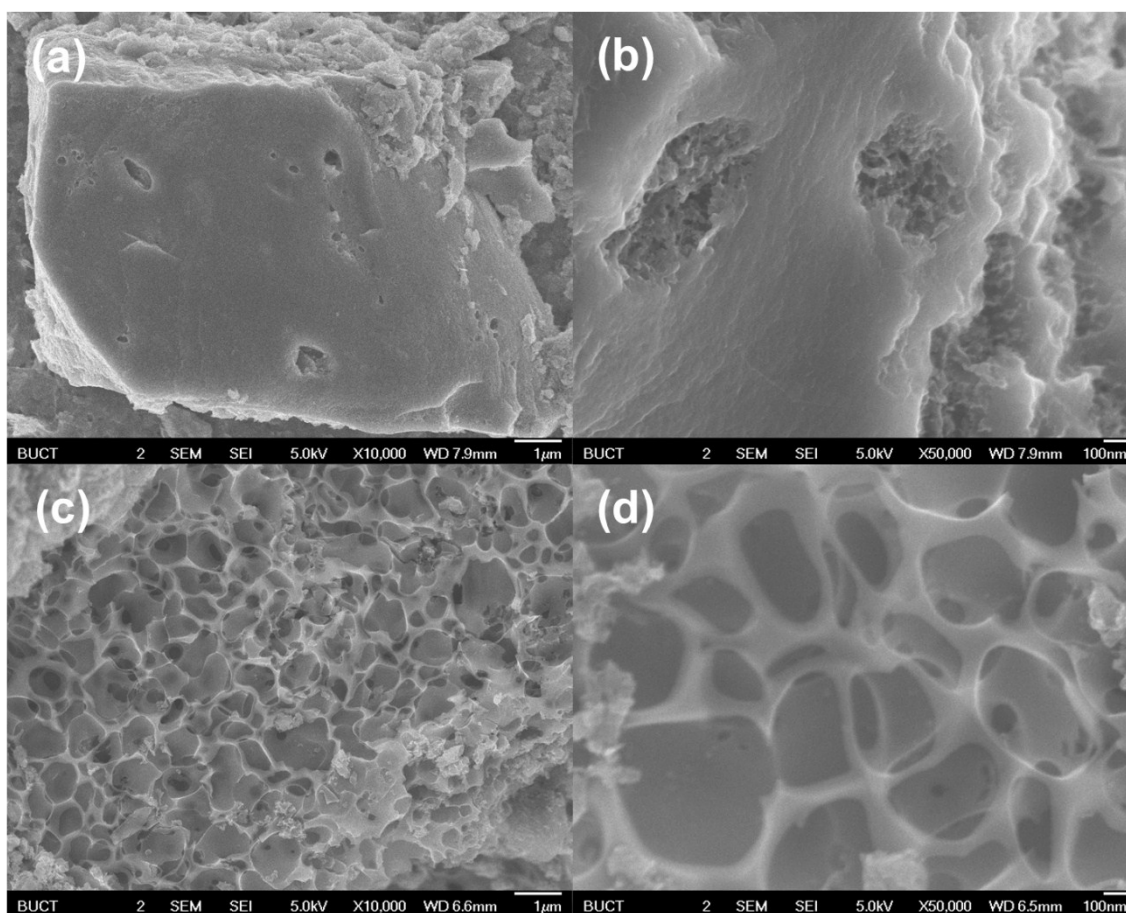


Fig. S1 Typical SEM images of the (a-b) NC (carbonized porphyra without KOH-activation) and (c-d) NHPC samples.

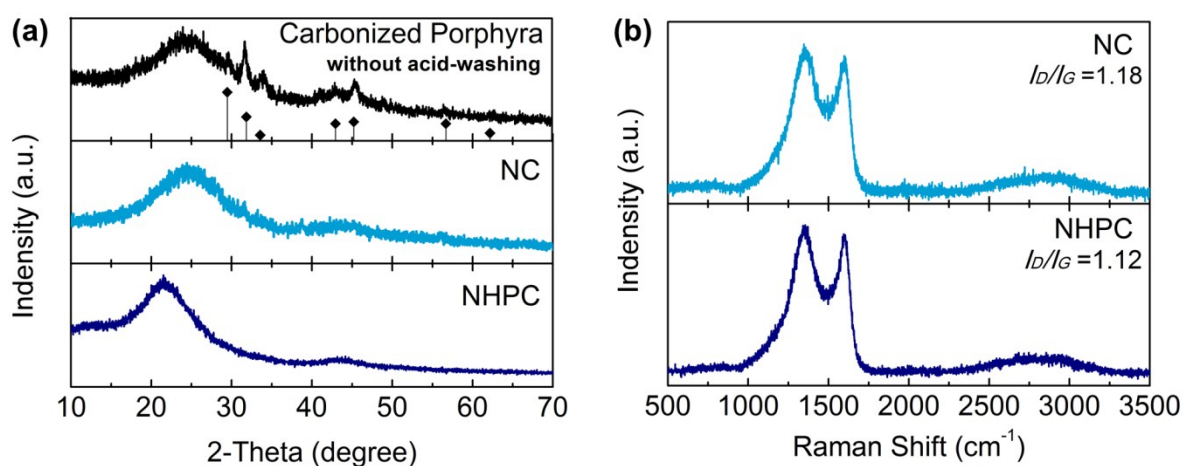


Fig. S2 a) XRD patterns of carbonized porphyrin (without KOH-activation and acid-washing), NC and NHPC. The characteristic peaks of carbonized porphyrin belong to calcium phosphate (JCPDS: no. 03-0604). b) Raman spectra of the NC and NHPC sample.

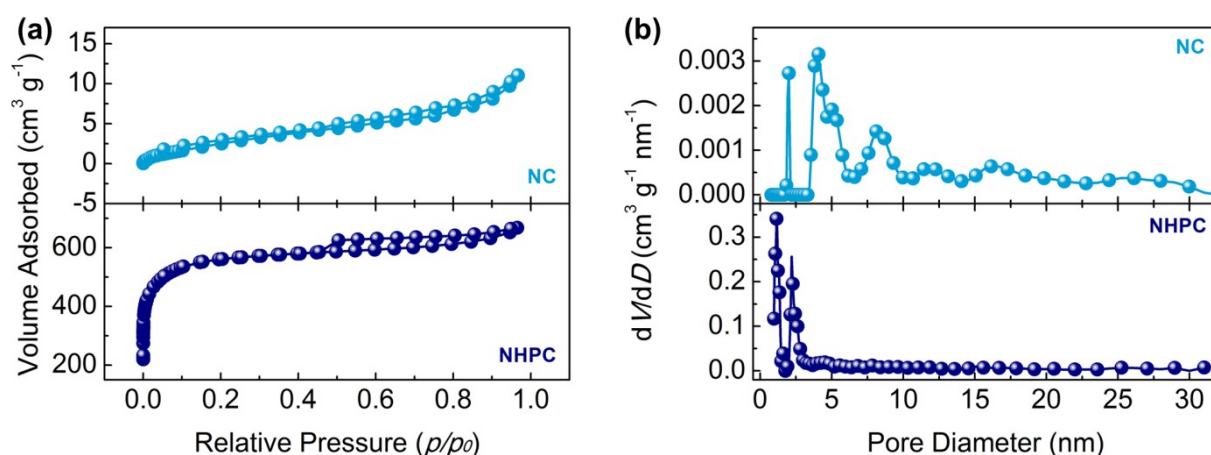


Fig. S3 BET characterization, a) nitrogen adsorption-desorption isotherm and b) corresponding DFT pore size distributions of NC and NHPC.

Table S2 BET characterization

Sample	S_{BET} (m^2/g)	S_{micro} (m^2/g)	S_{meso} (m^2/g)	Pore volume (cm^3/g)
NC	11.91	—	11.91	0.02
NHPC	2152.54	1972.38	180.16	1.05

3. Characterization of Fe-N_x/HPC

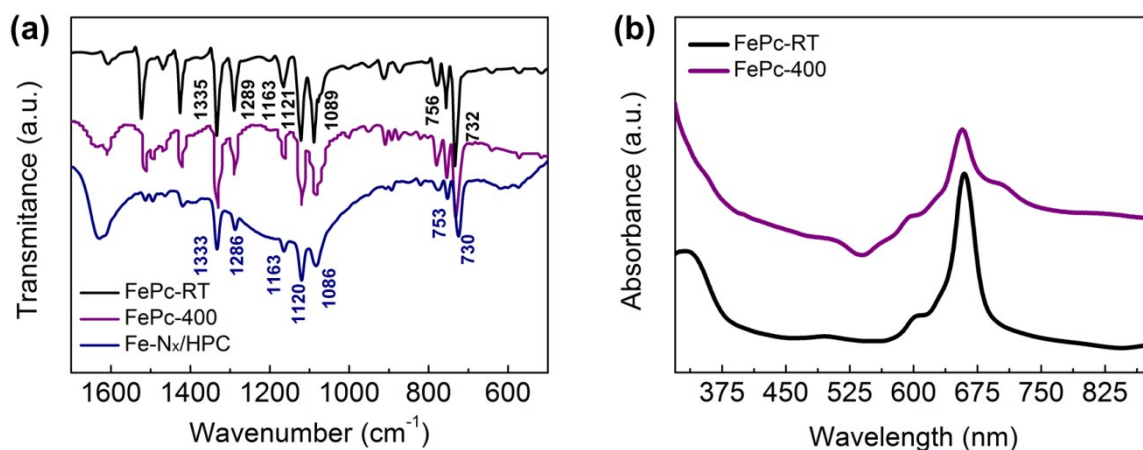


Fig. S4 a) FT-IR spectra of FePc-RT, FePc-400, Fe-N_x/HPC. b) UV spectra of FePc-RT and FePc-400. FePc-RT: FePc with room temperature; FePc-400: FePc heated at 400 °C heated at 400 °C for 2 h in an Ar atmosphere.

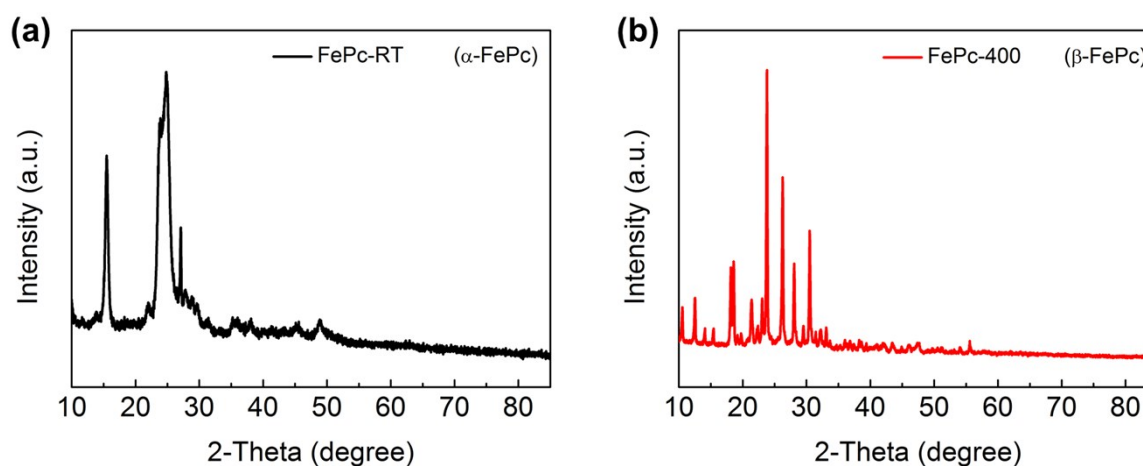


Fig. S5 XRD patterns of a) FePc-RT and b) FePc-400.

Table S3 The C-, N-, O- and Fe-content of NHPC, Fe-N_x/HPC and Fe-N_x/Vulcan. The capacitance of four C moieties, three N moieties and two Fe moieties of the above three samples.

Sample	Surface chemistry (XPS)			
	C (at %)	N (at %)	O (at %)	Fe (at %)
NHPC	81.59	2.13	16.28	—
Fe-N _x /HPC	85.31	5.51	8.82	0.35
Fe-N _x /Vulcan	85.08	3.53	11.12	0.27
Sample	Functionality (% of total C 1s)			
	C=C	C-N	C-O	—COOH
NHPC	48.9	19.6	16.5	15
Fe-N _x /HPC	42.9	25.7	17.1	14.3
Fe-N _x /Vulcan	52.1	23	13	11.9
Sample	Functionality (% of total N 1s)			
	pyridinic N	pyrrolic N	graphitic N	
NHPC	—	38.4	61.6	
Fe-N _x /HPC	25.5	46.4	28.1	
Fe-N _x /Vulcan	35.7	28.3	36	
Sample	Functionality (% of total Fe 2p)			
	Fe (II)	Fe (III)		
NHPC	—	—		
Fe-N _x /HPC	65.1	28		
Fe-N _x /Vulcan	74.7	14.7		

4. Catalytic performance for ORR

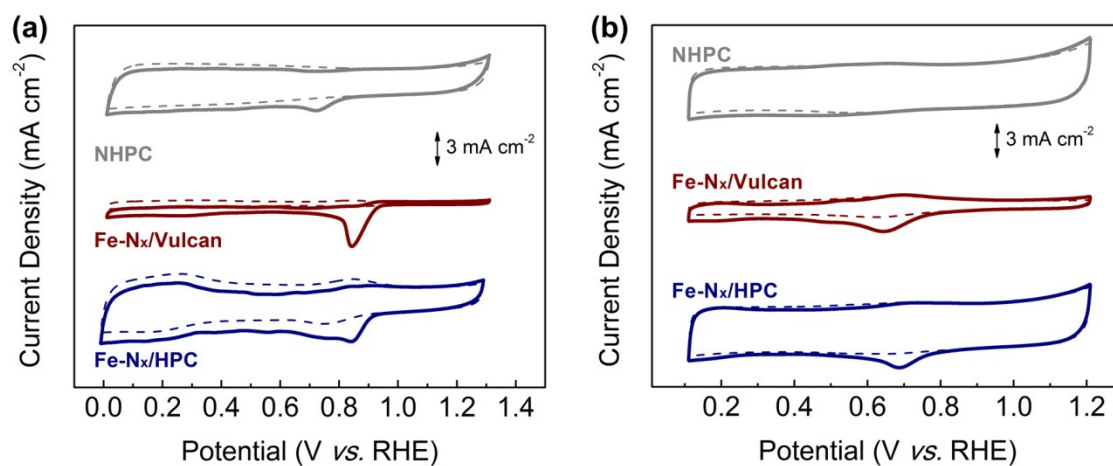


Fig. S6 CV curves of the NHPC, Fe-N_x/Vulcan and Fe-N_x/HPC electrodes in O₂-saturated (solid line) or N₂-saturated (dashed line) in a) 0.1 M KOH and b) 0.05 M H₂SO₄ at a sweep rate of 50 mV s⁻¹.

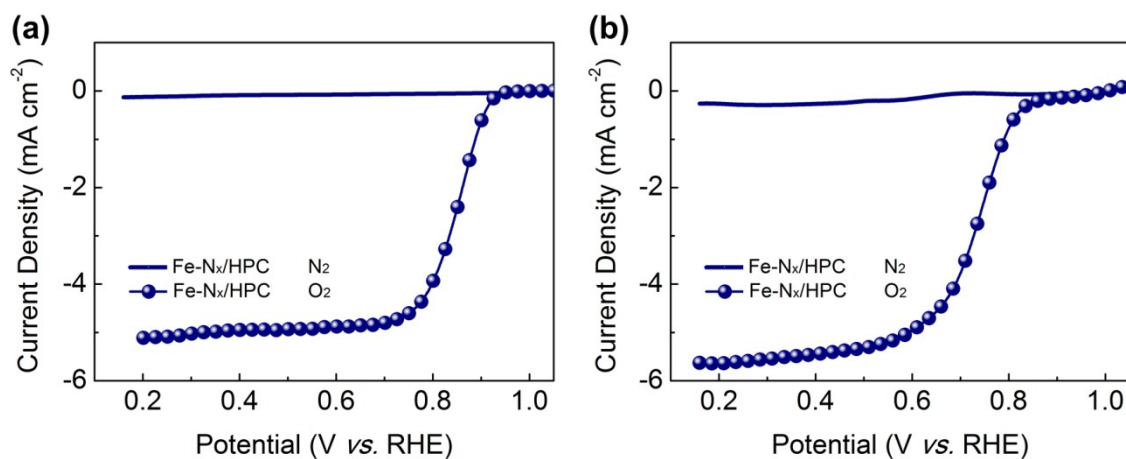


Fig. S7 RDE polarization curves of the Fe-N_x/HPC in O₂-saturated (symbol+line) or N₂-saturated (solid line) in a) 0.1 M KOH solution and b) 0.05 M H₂SO₄ with a sweep rate of 5 mV s⁻¹ at 1600 rpm.

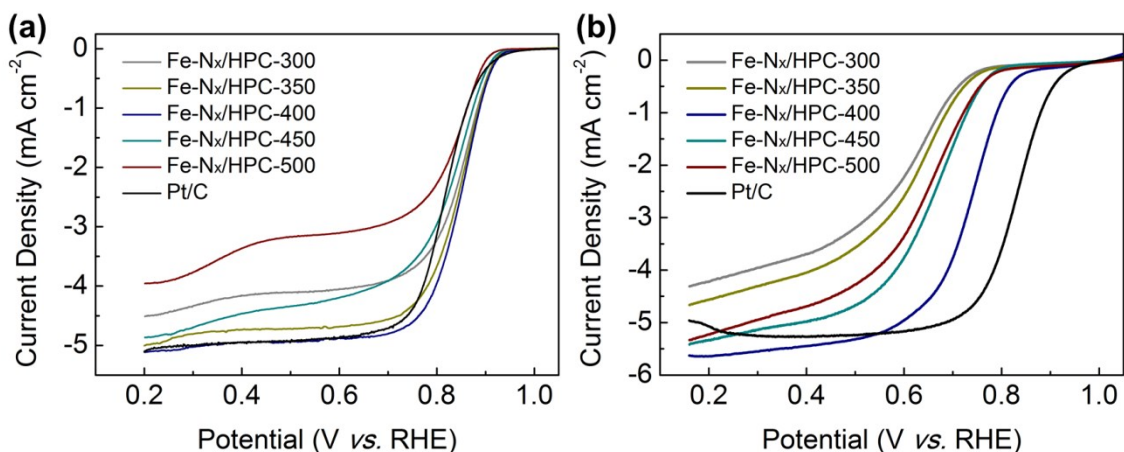


Fig. S8 RDE polarization curves of the Fe-N_x/HPC electrocatalysts with different temperature (300, 350, 400, 450 and 500 °C) heat treatment in O₂-saturated 0.1 M KOH solution with a sweep rate of 5 mV s⁻¹ at 1600 rpm.

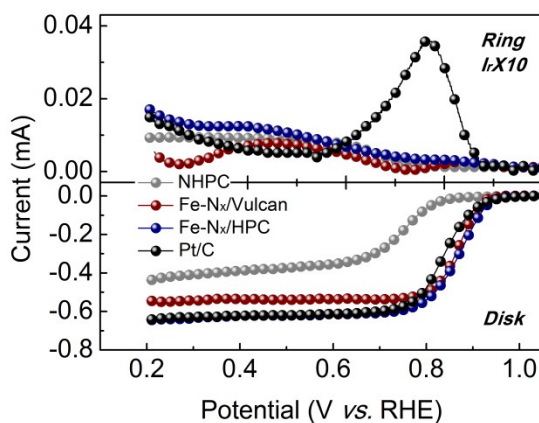


Fig. S9 RRDE voltammograms polarization curves of the NHPC, Fe-N_x/Vulcan, Fe-N_x/HPC and 20% Pt/C electrocatalysts O₂-saturated 0.1 M KOH solution at 1600 rpm. The disk current (I_d) is shown on the lower half and the ring current (I_r) is shown on the upper half of the graph. The disk potential was scanned at 5 mV s⁻¹, and the ring potential was constant at 1.5 V vs. RHE.

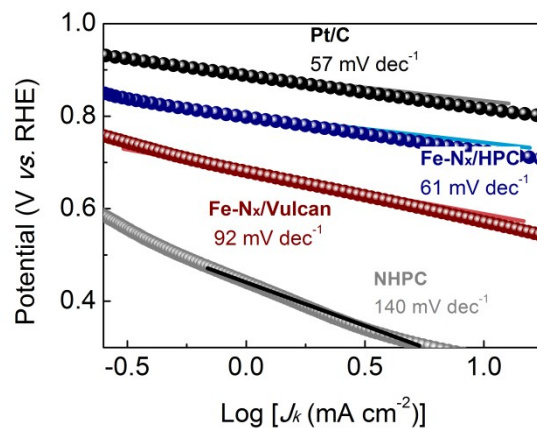


Fig. S10 Tafel plots in the acidic electrolyte of the NHPC, Fe-N_x/Vulcan, Fe-N_x/HPC and 20% Pt/C electrocatalysts derived by the mass-transport correction of corresponding RDE data.

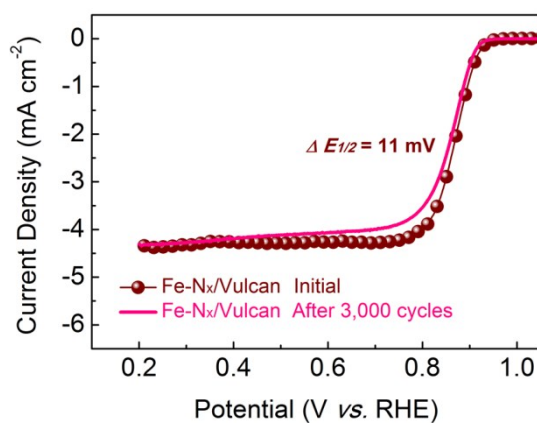


Fig. S11 Accelerated durability test, the ORR polarization curves of the Fe-N_x/Vulcan catalysts in O₂-saturated 0.1 M KOH solution before and after 3,000 potential cycles between 0.6 and 1.1 V.

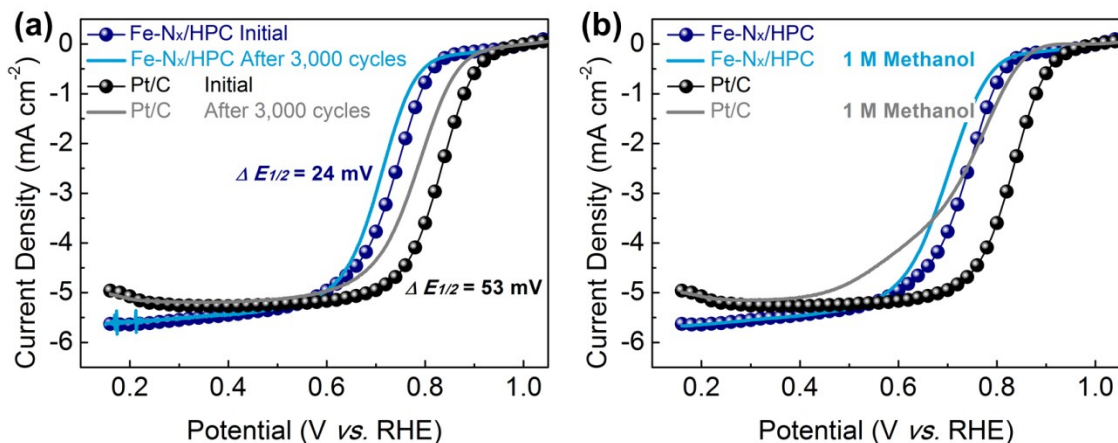


Fig. S12 a) Accelerated durability test, the ORR polarization curves of the Fe-N_x/HPC and 20% Pt/C electrocatalysts in O₂-saturated 0.05 M H₂SO₄ solution, before and after 3,000 potential cycles between 0.6 and 1.1 V. b) Methanol tolerance test, the ORR polarization curves of the Fe-N_x/HPC and 20% Pt/C electrocatalysts in O₂-saturated 0.05 M H₂SO₄, with or without 1 M methanol.

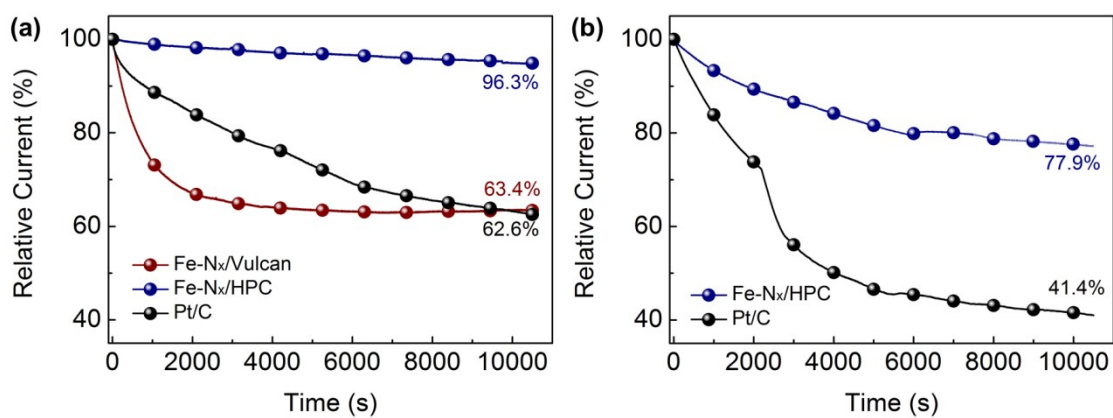


Fig. S13 Durability evaluation measured by the current *versus* time (*i-t*) chronoamperometric responses of a) the Fe-N_x/Vulcan, Fe-N_x/HPC and commercial Pt/C electrodes in the O₂-saturated 0.1 M KOH solution, and b) the Fe-N_x/HPC and commercial Pt/C electrodes in the O₂-saturated 0.05 M H₂SO₄ solution.

Table S1. Comparison of ORR performance in alkaline and acidic electrolyte for Fe-N_x/HPC with the reported Fe-N-C (derived from FePc) catalysts.

Catalyst	Loading mass ($\mu\text{g cm}^{-2}$)	Electrolyte	$E_{1/2}$ (V)	Sweep Rate (mV s^{-1})	Ref.
Fe-N _x /HPC	100	0.1 M KOH	0.88 vs. RHE	5	This work
	200	0.05 M H ₂ SO ₄	0.76 vs. RHE	5	
FePc-Py-CNT	318	0.1 M KOH	0.915 vs. RHE	10	[1]
	318	0.5 M H ₂ SO ₄	0.42 vs. Ag/AgCl	10	
α -FePc	210	0.5 M H ₂ SO ₄	0.62 vs. RHE	5	[2]
β -FePc	210	0.5 M H ₂ SO ₄	0.60 vs. RHE	5	
Fe-SPc/KJ300	612	0.1 M HClO ₄	0.62 vs. RHE	10	[3]
Fe-N-C/VA-CNT	600	0.5 M H ₂ SO ₄	0.79 vs. RHE	10	[4]
Fe _{0.5} -950	818	0.1 M H ₂ SO ₄	0.9 vs. RHE	10	[5]
bi-FePc/GNS	400	0.5 M H ₂ SO ₄	-0.09 vs. Hg/Hg ₂ SO ₄	5	[6]
FePc/CB-EC600	100	0.1 M KOH	0.91 vs. RHE	5	[7]
N-Fe/G(100)-900	50	0.1 M KOH	0.81 vs. RHE	10	[8]
N-Fe/G(60)-900-S	500	0.1 M HClO ₄	0.716 vs. RHE	10	

[1] R. Cao, R. Thapa, H. Kim, X. Xu, M. G. Kim, Q. Li, N. Park, M. Liu and J. Cho, *Nat. Commun.*, 2013, 4, 2076.

[2] S. Baranton, C. Coutanceau, E. Garnier and J. M. Léger, *Journal of Electroanalytical Chemistry*, 2006, 590, 100-110.

[3] W. Li, A. Yu, C. H. Drew, G. L. Bernard and Z. Chen, *J. Am. Chem. Soc.*, 2010, 132, 17056–17058.

[4] S. Yasuda, A. Furuya, Y. Uchibori, J. Kim and K. Murakoshi, *Adv. Funct. Mater.*, 2016, 26, 738-744.

[5] A. Zitolo, V. Goellner, V. Armel, M. T. Sougrati, T. Mineva, L. Stievano, E. Fonda and F. Jaouen, *Nat. Mater.*, 2015, 14, 937-942.

[6] T. Li, Y. Peng, K. Li, R. Zhang, L. Zheng, D. Xia and X. Zuo, *Journal of Power Sources*, 2015, 293, 511-518.

[7] S. Zhang, H. Zhang, X. Hua and S. Chen, *J. Mater. Chem. A*, 2015, 3, 10013-10019.

[8] Q. Lai, Q. Gao, Q. Su, Y. Liang, Y. Wang and Z. Yang, *Nanoscale*, 2015, 7, 14707-14714.